Making polymeric micro- and nanoparticles of complex shapes

Julie A. Champion, Yogesh K. Katare, and Samir Mitragotri*

Department of Chemical Engineering, University of California, Santa Barbara, CA 93106

Polymeric micro- and nanoparticles play a central role in varied applications such as drug delivery, medical imaging, and advanced materials, as well as in fundamental studies in fields such as microfluidics and nanotechnology. Functional behavior of polymeric particles in these fields is strongly influenced by their shape. However, the availability of precisely shaped polymeric particles has been a major bottleneck in understanding and capitalizing on the role of shape in particle function. Here we report a method that directly addresses this need. Our method uses routine laboratory chemicals and equipment to make particles with >20 distinct shapes and characteristic features ranging in size from 60 nm to 30 μm. This method offers independent control over important particle properties such as size and shape, which is crucial to the development of nonspherical particles both as tools and products for a variety of fields.

morphology | nanotechnology | geometry | drug delivery | nonspherical

Fig. 1. Methods used for making particles with different shapes can be categorized into two general schemes. (*Upper*) Scheme A involves liquefaction of particles by using heat or toluene, stretching the film in one or two dimensions and solidifying the particles by extracting toluene or cooling. The example shown here produces elliptical disks. (*Lower*) Scheme B involves stretching the film in air to create voids around the particle, followed by liquefaction using heat or toluene and solidification. The example shown here produces barrels.

Polymeric particles are used in a diverse array of applications including drug delivery (1), advanced materials (2), personal care (3), and medical imaging (4). They also are used in fundamental studies in fields such as microfluidics (5) and nanotechnology (6). Particle shape is a critical parameter that can significantly influence particle function. The vast potential of shape, however, has not been fully explored due to difficulties in creating polymer particles with controlled shapes. Several reports exist on fabrication of polymeric particles with nonspherical geometries. These approaches make use of self-assembly (7–9), photolithography (10), nonwetting template molding (11), microfluidics (12, 13), and stretching of spherical particles (14, 15). Collectively, these methods have produced particles of several distinct shapes. Some of these methods provide advantages such as scalability, high throughput, and precise control over particle shape. However, they also suffer from drawbacks including cost, particle size limitations, low throughput, and limited ability to sculpt particles in three dimensions. Accordingly, simple, versatile, inexpensive, and high-throughput methods of fabricating nonspherical particles still remain a bottleneck of future discoveries in a diverse array of fields. Here, we report a simple method that generates particles of >20 distinct shapes in large, reproducible quantities.

Results

Spherical polystyrene (PS) particles of diameters between 60 nm and 10 μm are used here as a starting material for preparing particles of complex shapes. These particles are suspended in an aqueous solution of polyvinyl alcohol (PVA) and cast into films (14), which are then manipulated to engineer particle shape. The method for engineering shape can be classified into two general approaches (Fig. 1). In the first approach, termed scheme A, PS particles are liquefied by using solvent or by heating above the glass transition temperature (T_g) of PS and then stretched in one or two dimensions. In the second approach, scheme B, PVA films are stretched first to create voids around the particles. These voids then are filled by liquefying the particles using solvent or heat. Resolidifying the particles after manipulation, by solvent extraction or cooling, sets their new shape. Finally, the particles
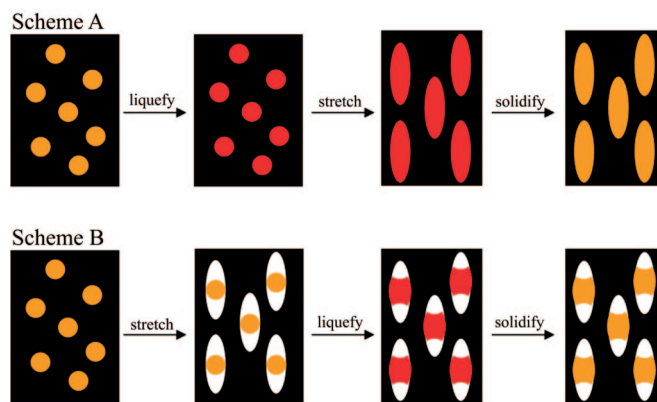
are collected by dissolving the film. Here we report a surprising finding that these two approaches, although apparently simple, can give rise to an incredibly diverse range of particle shapes. Final particle shape is dictated by the material properties of the film (T_g and thickness), the material properties of the particles (T_g and viscosity), interactions between particles and film (adhesion strength), and the stretching parameters (extent and dimensionality). A detailed summary of parameters leading to each shape is provided in supporting information (SI) Tables 1–3. Particle volume remains constant during stretching, governed entirely by the volume of the initial sphere. Thus, size and shape of particles can be independently controlled.

Particles made by using scheme A are shown in Fig. 2. These particles share the same general mechanism of formation: the liquefied particle is stretched due to its strong association with the film arising from hydrogen bonding. However, the final shape depends strongly on the details of key parameters. For example, stretching particles in a thin film (35 μm) produces flatter particles [Fig. 2b, length/width aspect ratio (AR_{LW}) = 6.1, width/thickness aspect ratio (AR_{WT}) = 2.0], whereas stretching in a thicker film (70 μm) produces rods with a nearly circular cross-section where width and thickness are approximately equal

Fig. 2. Micrographs of shapes made by using scheme A. (*a*) Spheres. (*b*) Rectangular disks. (*c*) Rods. (*d*) Worms. (*e*) Oblate ellipses. (*f*) Elliptical disks. (*g*) UFOs. (*h*) Circular disks. (Scale bars: 2 μm.)

(Fig. 2*c*; $AR_{LW} = 2.6, AR_{WT} = 1.1$). The ends of rectangular disks (Fig. 2*b*) and cylindrical rods (Fig. 2*c*) are relatively flat owing to the high viscosity of liquefied droplet, which in turn can be attributed to the use of low temperatures used for liquefaction (120°C). Increasing the liquefaction temperature, decreasing the viscosity, created sharp-ended worm-like particles with nearly circular cross-sections (Fig. 2*d*; $AR_{LW} = 14.1, AR_{WT} = 1.2$). The exact tortuosity of worms varied from particle to particle. Two dimensional (2D) stretching of heat-liquefied particles led to oblate ellipsoids with aspect ratios dictated by the extent of stretching (Fig. 2*e*; $AR_{WT} = 3.6$).

Replacing heat with toluene, as a mode of liquefying particles, led to entirely different shapes due to decreased PS viscosity. Specifically, 1D stretching of films after toluene-liquefaction formed very thin elliptical disks with curved ends (Fig. 2*f*; $AR_{LW} = 4.4$, $AR_{WT} = 10.5$) under conditions where heat-liquefied particles formed rectangular disks with blunt ends and lower AR_{WT} values. Peculiar results were obtained when toluene-liquefied particles were stretched in 2D. Moderate stretching of toluene-liquefied particles led to UFO-like particles (Fig. 2*g*) due to preferential stretching of the particle around the equator. Extensive stretching under the same conditions or comparable stretching of smaller particles, however, eliminated the dome and produced flat circular disks (Fig. 2*h*; $AR_{WT} = 8.7$). Although the circular disks and oblate ellipsoids in Fig. 2 *e* and *h* have approximately the same diameter, the circular disks are much thinner, with an AR_{WT} 2.4 times larger than that for oblate ellipsoids.

More complex shapes were made by using scheme B. Conducting 1D stretching of the film without particle-liquefaction creates an ellipsoidal void around the particle. Upon heat-induced liquefaction, PS fills the void by wetting the film. However, at relatively low liquefaction temperatures (130°C), the high viscosity of PS inhibits complete filling of the void and leads to barrel-like particles upon solidification (Fig. 3*a*; *Inset* shows concave regions at both ends). Interestingly, liquefaction at higher temperatures (140°C), keeping all other parameters the same, decreases PS viscosity, and induces distribution of PS predominantly to one end of the void, increasing the contact area between PS and PVA, and forms bullet-like structures (Fig. 3*b*). Once again, replacing heat with toluene as a means of liquefaction, after dry-stretching of film produced different shapes due to further reduction of viscosity. Conducting 1D stretching in air followed by toluene-induced liquefaction formed pill-like particles (Fig. 3*c*). Moderate 2D stretching of the film in air followed by toluene-induced liquefaction led to pulley-shaped particles (Fig. 3*d*, a circular disk with a groove in the middle; *Inset* shows side view). Repeating the same procedure with extensive stretch-

ing produced biconvex lenses (Fig. 3*e*; *Inset* shows side view). As the complexity of shape increases, the definitions for characterizing shape become unclear. Shape parameters that are more complex than aspect ratios will need to be defined based on the critical shape features for given applications.

Combination and/or repetition of schemes A and B led to even more unusual shapes including ribbon-like particles with curled ends (Fig. 4*a*; *Inset* shows a curl), bicones (Fig. 4*b*), diamond disks (Fig. 4*c*), emarginate disks (Fig. 4*d*), flat pills (Fig. 4*e*), elongated hexagonal disks (Fig. 4*f*), ravioli (Fig. 4*g*), and tacos (Fig. 4*h*) (see SI Tables 1–3 for detailed procedures for each shape).

The method reported here can be further modified to control additional design features, such as surface texture, while keeping size and shape constant. For example, scheme B was modified to make wrinkled prolate ellipsoids (Fig. 4*i*). In this modification,
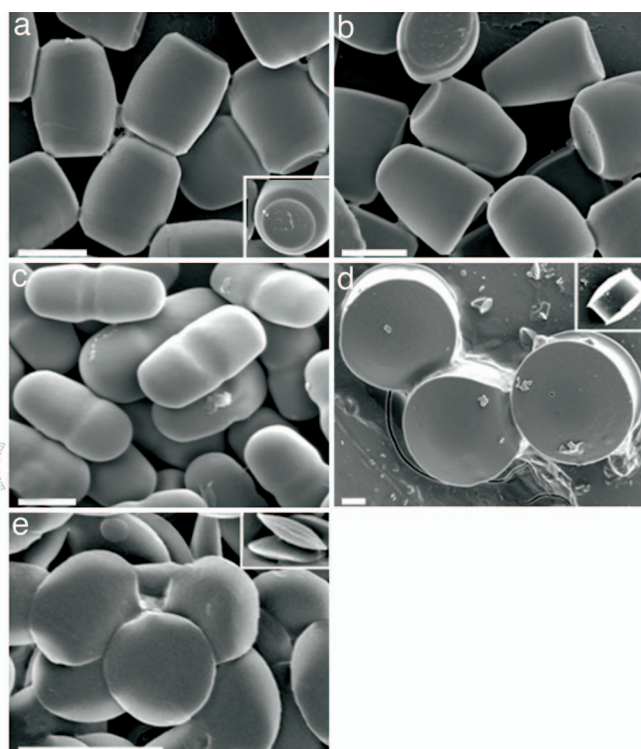
Fig. 3. Micrographs of shapes made by using scheme B. (*a*) Barrels. (*b*) Bullets. (*c*) Pills. (*d*) Pulleys. (*e*) Biconvex lenses. (Scale bars: 2 μm.)
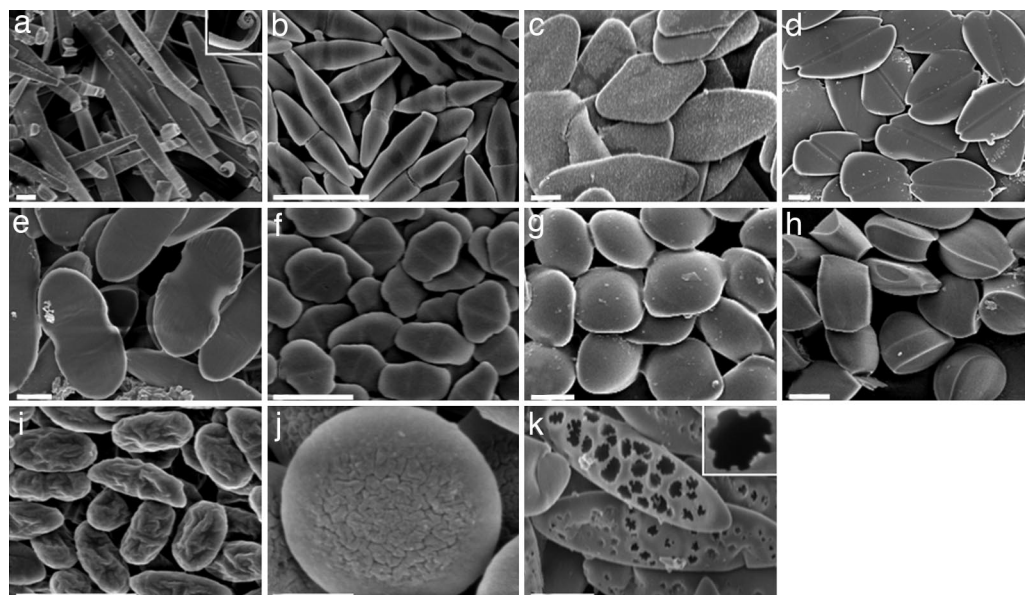
Fig. 4. Micrographs of shapes made by using combinations of schemes A and B. (*a*) Ribbons with curled ends. (*b*) Bicones. (*c*) Diamond disks. (*d*) Emarginate disks. (*e*) Flat pills. (*f*) Elongated hexagonal disks. (*g*) Ravioli. (*h*) Tacos. (*i*) Wrinkled prolate ellipsoids. (*j*) Wrinkled oblate ellipses. (*k*) Porous elliptical disks. (Scale bars: 2 μm, *a–i* and *k*; 400 nm, *j*.)

the film was stretched while keeping the particles solid, and it was removed from the stretcher before particle liquefaction. This allowed the film to relax and produced wrinkles at the film–void interface. Subsequent toluene-induced liquefaction produced particles shown in Fig. 4*i*. A similar procedure performed by 2D stretching produced wrinkled oblate ellipsoids (Fig. 4*j*). In another example, porous elliptical disks (Fig. 4*k*) were formed when toluene-liquefied particles, stretched according to scheme A, were immediately immersed in isopropanol to remove toluene, omitting the air-drying step. This led to rapid removal of toluene from the particle and created holes in one side of the particle surface.

Discussion

The method reported here generates particles of incredibly diverse shapes. The resultant shapes can be explained by the physical properties of the particles and film and the interaction between them. Scheme A generally leads to simpler shapes because fewer properties, primarily particle viscosity and film thickness, are relevant to the final shape. Particle viscosity, for example, dictates whether a shape will have pointy ends (worms, elliptical disks) or flatter ends (rectangular disks, rods). Higher viscosity of particles (arising from stretching at low temperature) prevents the film from stretching to a sharp point due to preservation of width of the particle during stretching. Regardless of viscosity, thinner films led to creation of flatter particles and vice versa. Scheme B leads to generally more complex shapes because of the introduction of an additional design parameter in the form of particle-film wetting properties. In particular, the interplay between particle-film wetting properties and particle viscosity introduced further diversities in shape.

The shapes reported here represent a wide range of geometries including predominantly 1D (e.g., worms), 2D (e.g., elliptical and circular disks), and 3D (e.g., UFO and barrels). In addition, particles also display regions of varying concavity, curvature, aspect ratio, and surface texture. Shapes described here were made primarily from 1- to 5-μm particles (original sphere diameters of particles in Figs. 2–4 are listed in SI Tables 1–3). However, the method has been easily extended to nanoparticles (Fig. 5), which will increase the possible applications. Using the procedures described here, it is possible to make a group of particles where important properties such as volume, shape, surface area, curvature, and texture can be systematically and independently varied. Such particles will be crucial in methodically identifying the role of geometric parameters in particle function in a variety of fields.

It is remarkable that a diverse range of particles can be made by such a simple method. Diversity can be further enhanced by using more complex starting materials, for example hollow microspheres, or by using additional forces, such as magnetic forces, to further manipulate the particles. The method described here offers a powerful tool for fabricating particles of various shapes. It can be adopted to prepare particles from polymers other than PS, for example, biodegradable poly(lactic-co-glycolic acid) (data not shown) and poly(methyl methacrylate) (16). The method is also amenable to scale up through increased particle loading in films, increased film thickness, parallel processing, and automation. Currently with small bench-scale production, a single stretcher makes 10^8 to 10^{12} particles, depending on particle size.

The method reported here will facilitate fundamental research and development of new applications in various disciplines. There is already initial evidence supporting the importance of shape in various scientific and technological applications, such as in the design of new carriers for drug delivery (17–19). Avoid-
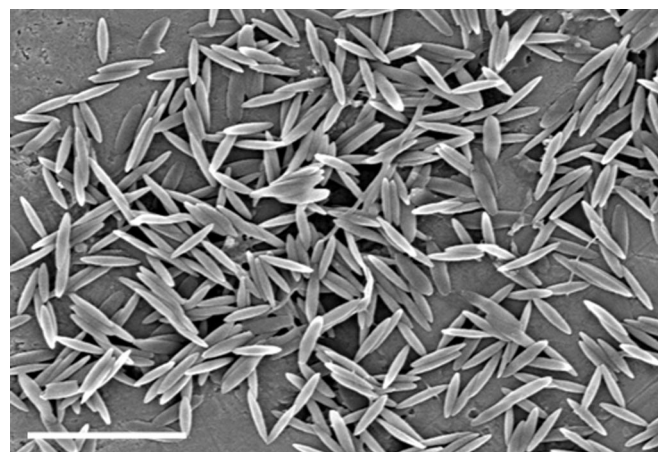
Fig. 5. Micrograph of elliptical disks made from 220-nm-diameter PS spheres. (Scale bar: 2 μm.)

ENGINEERING

ance of uptake by immune cells is essential to the survival of drug delivery carriers in the human body and is known to be sensitive to their shape (20). There is also evidence that the most basic function of particles, degradation to release therapeutic molecules, depends on particle shape (21). Nonspherical particles that have flat faces could provide zero-order release, whereas particles with regions of different thicknesses could offer unique degradation profiles because the shape of the particle will change over time. Particle shape will also influence targeting ability, in particular how well particles attach to target cells and remain attached, especially in the presence of flow (17). One important limitation of this shape manipulation method for drug delivery applications is exposure of encapsulated proteins and other biological therapeutics to solvent. This could be reduced by the addition of stabilizing molecules, which shield the aqueous phase from solvent (22), or by using hydrophilic biodegradable polymer particles, instead of the more traditional hydrophobic ones, and stretching them in a hydrophobic polymer film. In addition, heat stretching can be used instead of solvent, and several biodegradable polymers have low T_g values [for example, poly(lactic-co-glycolic acid) $T_g = 40-60°C$].

In addition to drug delivery, this method of shape manipulation can significantly contribute to a broad variety of other fields. The wealth of nano- and microscale shapes in nature, from spiral-shaped bacteria to the peculiar shapes of platelets and erythrocytes, hints at the importance of shape in biology. Availability of polymeric particles with distinct shapes will prove to be a useful tool in uncovering the role of shape in various biological systems. Particles can be used as models for similar-looking objects, such as bacteria, not only in biological applications but also in environmental fields to study bacterial migration in soil or water. In a completely unrelated field, nonspherical particles also may open new applications in advanced materials due to their unique scattering and packing properties (23). Nonspherical particles also can be used as research tools or probes in rheology or aerodynamics or as sensors in microrheology studies. The uses and knowledge gained from particles with defined shapes seem limitless, and the availability of a simple method to make such particles will catalyze many new discoveries and technologies.

Methods

Film Preparation. Un-cross-linked PS spherical particles (radii 30 nm to 5 μm) were purchased from Polysciences (Warrington, PA). PVA was purchased from Sigma Chemicals (St. Louis, MO). We dissolved 5–10% PVA (2–4 g in 40 ml of water) in 85°C water, depending on the desired film thickness. Then, 2% (wt/vol) glycerol was added to plasticize and reduce the T_g of some films. Spherical particles were added to this mixture at a concentration of 0.04–0.7% (wt/vol), and the films were dried on a 19- $\times$ 24.5-cm flat surface to thicknesses of 35 μm for 5% PVA and 70 μm for 10% PVA. Films dried in ≈18 h. In some cases, the film was reinforced after one round of liquefaction and stretching. For this purpose, the film was laid on a solution of 5% PVA, and the PVA solution also was poured on top of the film. The solution was allowed to dry for 24 h.

Film Stretching. The film was typically cut into sections of 5 × 5 cm and mounted on the stretchers. The 1D stretcher comprised two aluminum blocks mounted on a screw, which when turned separates the blocks. The 2D stretcher was similar in design, except that it consisted of two pairs of orthogonal blocks that move simultaneously. The film was stretched in 1D or 2D in air, hot oil, or toluene. All stretching was performed at a rate of 0.3–0.5 mm/s. In cases of heat-stretching, the film was immersed in hot oil for 5 min and stretched while still in the oil. The temperature of the oil was controlled between 120°C and 150°C depending on the desired shape. If films were stretched before heating, they were heated for 12 min. In both cases the film was removed and allowed to cool in air for 30 min. In cases of toluene-stretching, the film was immersed in toluene for 3 h regardless of whether stretching occurred before or after. After toluene immersion, the film was removed, air-dried for 10 h, and soaked in isopropanol for 12 h to extract residual toluene. To induce formation of holes in particles, air drying was omitted, and films were placed directly in isopropanol from toluene. The extent of stretching was varied from as little as 1.1-fold to as much as 11-fold, depending on the objective. On several occasions, the film was stretched sequentially in multiple dimensions or multiple times in the same dimension. The detailed conditions used for each shape are listed in SI Tables 1–3.

Particle Recovery. The films were dissolved in 30% isopropanol/ water at 65°C. The particles were washed by centrifugation with the same solution 10 times to remove all PVA from the surface of the particles. To verify particle morphology, particles were coated with palladium (Hummer 6.2 Sputtering System; Anatech Ltd., Union City, CA) and imaged with a Sirion 400 scanning electron microscope (FEI Co., Hillsboro, OR) at 3 eV. Particle dimensions were measured from the micrographs with Metamorph image acquisition and analysis software (Universal Imaging Systems, Downingtown, PA).

1. Stolnik S, Illum L, Davis SS (1995) *Adv Drug Delivery Rev* 16:195–214.
2. Subramanian G, Manoharan VN, Thorne JD, Pine DJ (1999) *Adv Mater* 11:1261–1265.
3. Luppi B, Cerchiara T, Bigucci F, Basile R, Zecchi V (2004) *J Pharm Pharmacol* 56:407–411.
4. Chen HH, Le Visage C, Qiu BS, Du XY, Ouwerkerk R, Leong KW, Yang XM (2005) *Magn Reson Med* 53:614–620.
5. Mason TG, Ganesan K, vanZanten JH, Wirtz D, Kuo SC (1997) *Phys Rev Lett* 79:3282–3285.
6. Andrea BR, Mayer JEM (1997) *J Polym Sci B* 35:1207–1216.
7. Manoharan VN, Elsesser MT, Pine DJ (2003) *Science* 301:483–487.
8. Yin YD, Xia YN (2001) *Adv Mater* 13:267–271.
9. Velev OD, Lenhoff AM, Kaler EW (2000) *Science* 287:2240–2243.
10. Dendukuri D, Pregibon DC, Collins J, Hatton TA, Doyle PS (2006) *Nat Mater* 5:365–369.
11. Rolland JP, Maynor BW, Euliss LE, Exner AE, Denison GM, DeSimone JM (2005) *J Am Chem Soc* 127:10096–10100.
12. Xu SQ, Nie ZH, Seo M, Lewis P, Kumacheva E, Stone HA, Garstecki P, Weibel DB, Gitlin I, Whitesides GM (2005) *Angew Chem Int Ed* 44:724–728.
13. Dendukuri D, Tsoi K, Hatton TA, Doyle PS (2005) *Langmuir* 21:2113–2116.
14. Ho CC, Keller A, Odell JA, Ottewill RH (1993) *Colloid Polym Sci* 271:469–479.
15. Lu Y, Yin YD, Xia YN (2001) *Adv Mater* 13:271–274.
16. Mohraz A, Solomon MJ (2005) *Langmuir* 21:5298–5306.
17. Decuzzi P, Ferrari M (2006) *Biomaterials* 27:5307–5314.
18. Geng Y, Dalhaimer P, Cai S, Tsai R, Tewari M, Minko T, Discher D (2007) *Nat Nanotechnol* 2:249–255.
19. Euliss LE, DuPont JA, Gratton S, DeSimone J (2006) *Chem Soc Rev* 35:1095–1104.
20. Champion JA, Mitragotri S (2006) *Proc Natl Acad Sci USA* 103:4930–4934.
21. Hsieh DST, Rhine WD, Langer R (1983) *J Pharm Sci* 72:17–22.
22. Manning MC, Patel K, Borchardt RT (1989) *Pharm Res* 6:903–918.
23. Manoharan VN, Pine DJ (2004) *Mater Res Soc Bull* 29:91–95.